Forsch Ingenieurwes
https://doi.org/10.1007/s10010-023-00630-5

ORIGINALARBEITEN/ORIGINALS

Influence of drivetrain efficiency determination on the torque control of wind turbines

M. Zweiffel[1] · G. Jacobs[1] · Z. Song[2] · P. Weidinger[2] · T. Decker[1] · J. Röder[1] · D. Bosse[1]

Received: 9 November 2022 / Accepted: 19 January 2023

Abstract

Decreasing the levelized cost of energy is a major design objective for wind turbines. Accordingly, the control is generally optimized to achieve a high energy production and a high-power coefficient. In partial load range, speed and torque are controlled via the generator torque but the rotor torque determines the power coefficient of the turbine. High uncertainties for the uncalibrated low-speed shaft torque measurement and varying drivetrain efficiencies which depend on the speed, load and temperature lead to a torque control error that reduces the power coefficient of the wind turbine. In this paper the rotor torque control error and the impact on the power coefficient of wind turbines is quantified. For this purpose, the variation of drivetrain efficiency is analyzed. An efficiency model for the wind turbine drivetrain is build and validated on the test bench. Then, the influence of the drivetrain speed, torque loads, non-torque loads, and temperature on the efficiency is quantified. Finally, the influence of the rotor torque control error on the power coefficient was simulated with an aerodynamic model. The results show that of all examined influences only torque and temperature significantly impacting the efficiency leading to rotor torque control errors that reduce the power coefficient and consequently increase the levelized cost of energy. Improved efficiency measurement on WT test benches or drivetrain efficiency modelling can reduce the rotor torque control error and therefore decrease the LCOE.

✉ M. Zweiffel
maximilian.zweiffel@cwd.rwth-aachen.de

[1] Chair for Wind Power Drives (CWD) of RWTH Aachen, Aachen, Germany

[2] Physikalisch technische Bundesanstalt Braunschweig (PTB), Braunschweig, Germany

Published online: 20 March 2023

Analyse des Einflusses der Wirkungsgradbestimmung im Antriebsstrang auf die Drehmomentregelung von Windenergieanlagen

Zusammenfassung

Die Senkung der Stromgestehungskosten (levelized cost of energy – LCOE) ist das Hauptziel bei der Entwicklung von Windenergieanlagen (WEA). Entsprechend wird die Anlagenregelung dahingehend optimiert, dass eine hohe Energieausbeute und ein hoher Leistungsbeiwert erreicht wird. Hierzu wird im Teillastbereich der Betriebspunkt durch Triebstrangdrehzahl und Drehmoment, über das Gegenmoment am Generator geregelt. Bestimmend für den Leistungsbeiwert ist jedoch der Betriebspunkt (Drehzahl und Drehmoment) am Rotor, der durch den Wirkungsgrad des Triebstranges vom Generatorbetriebspunkt abweicht. Direkte Messungen des Rotordrehmoments weisen hierbei hohe Unsicherheiten durch fehlende Möglichkeiten zur Kalibrierung auf. Auch die Berechnung des Rotordrehmoments aus dem Generatormoment führt auf Grund des variierenden Wirkungsgrades in Abhängigkeit von Drehzahl, Last und Temperatur zu Ungenauigkeiten. Ungenauigkeiten bei der Bestimmung des Rotordrehmomentes verursachen einen Fehler bei der Regelung der Anlage. In diesem Beitrag wird daher der Fehler bei der Bestimmung des Rotordrehmomentes sowie dessen Auswirkung auf den Leistungskoeffizienten von WEA quantifiziert. Zu diesem Zweck werden zunächst die Unsicherheiten bei der Bestimmung des Antriebsstrangwirkungsgrads analysiert. Anschließend wurde ein Wirkungsgradmodell für den Antriebsstrang einer WEA erstellt und auf dem Systemprüfstand validiert. Auf Basis des Modells und der Prüfstandsversuche kann der Einfluss von Drehzahl, Drehmoment, nicht-torsionaler Lasten und Temperatur auf den Wirkungsgrad quantifiziert werden. Abschließend wird der Einfluss des Fehlers in der Regelung der Rotordrehmoments auf den Leistungskoeffizienten mit einem aerodynamischen Modell simuliert. Die Ergebnisse zeigen, dass das Drehmoment und die Temperatur einen signifikanten Einfluss auf den Wirkungsgrad und damit die Bestimmung des Rotordrehmomentes haben. Der Fehler bei der Drehmomentregelung des Rotors führt dabei zu einer Verringerung des Leistungskoeffizienten und folglich zu einer Erhöhung der LCOE. Verbesserte kalibrierte Wirkungsgradmessungen auf WEA-Systemprüfständen oder eine betriebspunktabhängige Modellierung des Antriebsstrangwirkungsgrads können den Fehler bei der Regelung des Rotordrehmoments verringern und somit die LCOE senken.

1 Introduction

A major design objective for wind turbines (WTs) is low levelized cost of energy (LCOE). LCOE can be reduced by keeping capital and operational expenditures constant and increasing the annual energy production (AEP). Accordingly, to achieve high AEPs the WT control is optimized

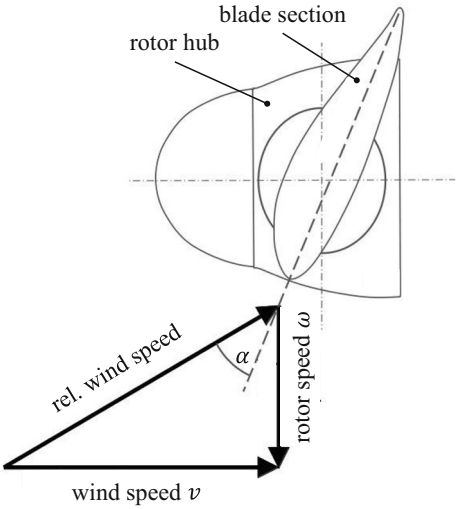

Fig. 1 Rotor aerodynamic according to [3]

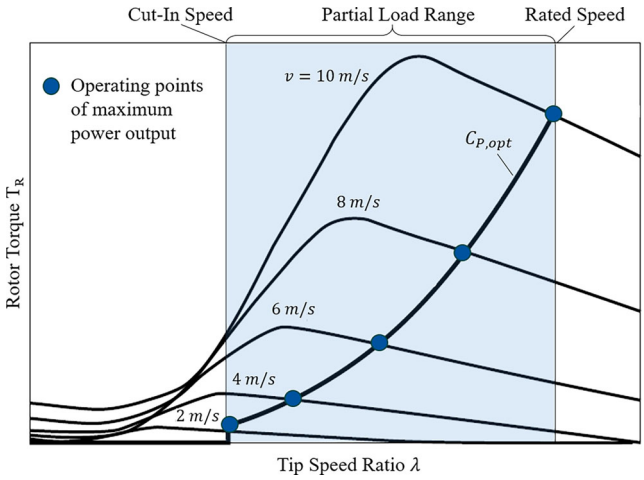

Fig. 2 Control curve for WT in the torque-speed map of the rotor, according to [4]

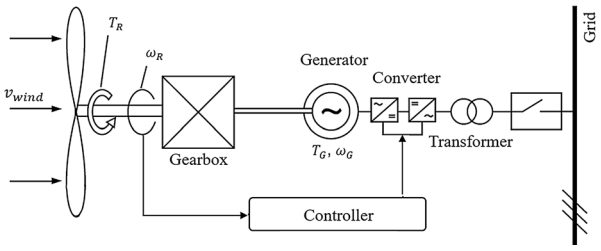

Fig. 3 Schematic OTC according to [6]

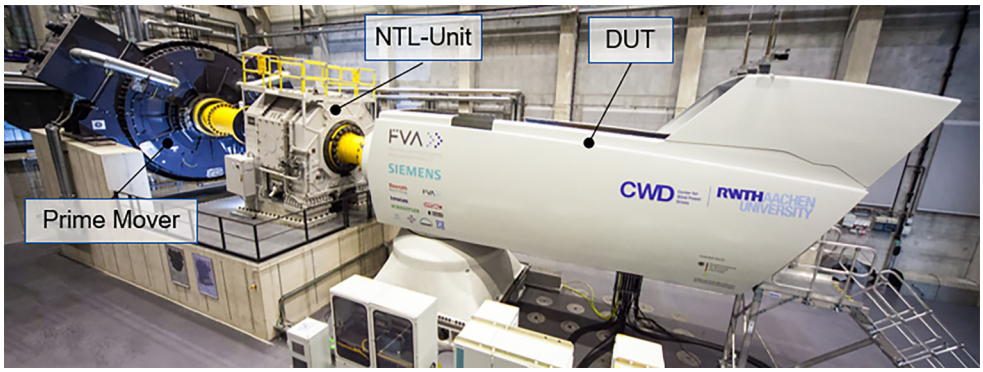

Fig. 4 FVA research nacelle at the CWD test bench

for maximum energy production in all wind conditions. At high wind speed, when the WT operates at nominal power, the power output is only limited by the maximum generator power and the efficiency of the rotor is actively reduced via blade pitching. In partial load operation, the power output is limited by the wind speed and an efficient energy conversion at the rotor is aimed [1]. The efficiency of the energy conversion from wind-speed v to output power P is described by the power coefficient, C_P and is calculated via Eq. 1 with the air density ϱ and the area of the rotor A [2].

$$C_P = \frac{P}{\frac{1}{2}\rho A v^3} \tag{1}$$

The power coefficient is dependent on the aerodynamics at the rotor blades. Figure 1. shows a simplified representation of the inflow angle of a blade section.

As can be seen, the inflow angle α, and the relative wind speed that is generating the aerodynamic force to turn the rotor is not only dependent on the wind speed v but also, the blade speed, that depends on rotor speed ω and rotor diameter R. Therefore, the tip-speed ratio λ is defined as:

$$\lambda = \frac{\omega \cdot R}{v} \tag{2}$$

Accordingly, the power coefficient C_P depends on λ. For each wind speed an optimal tip-speed-ratio λ_{opt} exists that leads to an optimal power coefficient $C_{P,opt}$. This is illustrated in Fig. 2.

Figure 2. shows the resulting $C_{P,opt}$ curve as function of rotor torque T_R and λ for different v. To achieve $C_{P,opt}$ in partial load range optimal torque control (OTC) is commonly used [5]. OTC represents a simple but effective method to run the WT close to the optimal operating point. The principle of OTC is shown schematically in Fig. 3.

With OTC only the shaft-speed ω_R is measured at the rotor or is derived from the electric quantities measured in the converter. However, the converter varies the electrical generator currents to set the generator torque T_G according to the shaft speed to reach optimal power coefficient $C_{p,opt}$.

In practical implementation the rotor torque is often approximated by merging Eq. 1 and 2 which leads to Eq. 3 and 4. $C_{p,opt}$ at rated torque and optimal tip-speed ratio λ_{opt} depend on the specific aerodynamic behavior and are determined for each WT individually [6].

$$T_G = c\omega^3 \tag{3}$$

With

$$c = \frac{1}{2}\rho\pi R^5 \frac{C_{p,\mathrm{opt}}}{\lambda_{\mathrm{opt}}{}^3} \tag{4}$$

As described above, T_G is the control variable, but the actual control-target is the rotor torque T_R, that can either be measured directly at the low-speed-shaft (LSS) or cal-

Table 1 Performance data of DUT

Nominal Power	2750 kW
Rotor Diameter	80 m
Res. Swept Area	5027 m^2
Max. Rotor Speed	17.5 rpm
Rated Torque	1550 kNm
Gear Ratio	62.775

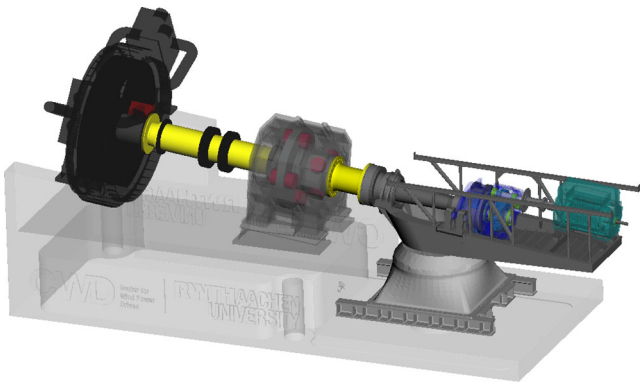

Fig. 5 MBS model of the wind turbine drivetrain on the 4 MW test bench

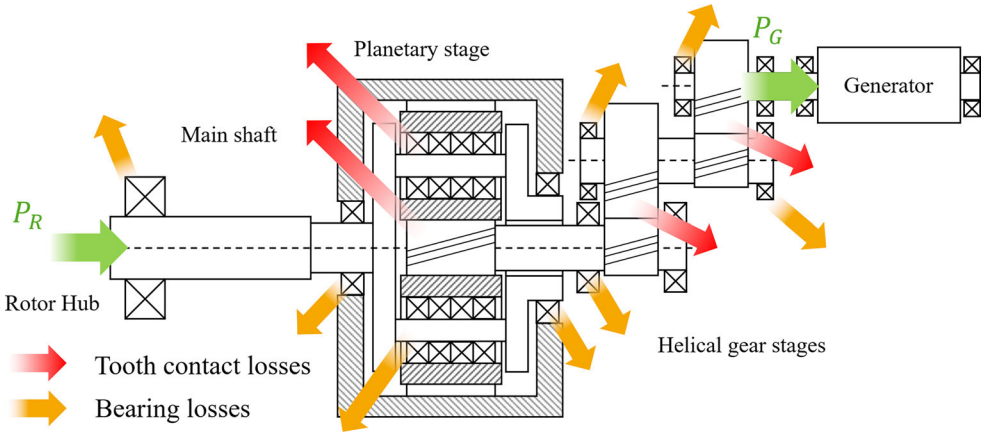

Fig. 6 Schematic illustration of the modelled drive train losses and the location

culated from T_G with the gear ratio and the drivetrain-efficiency. However, both approaches show significant errors.

On-site torque measurements can be performed with strain gauges at the LSS to measure T_G. In torque measurement based on strain gauges, material parameters such as Young's modulus and k-factor, and geometry of the deformation body and the strain gauges themselves are usually insufficient. A correct torque measurement with a defined uncertainty interval can be guaranteed by calibration. Currently, however, calibration is only possible up to 1.1 MNm. For a non-calibrated torque measurement using strain gauges, an accuracy of only 5–7% can be achieved [7]. With the help of calibrated torque sensors, torque <1.5 MNm on the LSS can be measured with an uncertainty $<0.5\%$.

In contrast to the rotor torque T_R, calibration procedures are feasible and standardized in the measuring range of the generator torque T_G. Calibration enables generator torque measurements with high accuracies of less than 0.1% [8]. To transfer the T_G to T_R, the drivetrain efficiency must be known. Existing approaches to calculate the efficiency of machine elements like gears and bearings determine the efficiency dependent on drivetrain loads as well as speed of rotation, and the viscosity of the lubricants. Nevertheless, efficiency calculations always show uncertainties too. Additionally, in practical use the efficiencies are often estimated as a constant value to calculate the rotor torque. Therefore, the scattering of the efficiency is neglected. Thus, it is to be expected that errors in rotor torque determination lead to control errors. These rotor torque control errors result in lower power coefficients and in lower AEP leading to higher LCOE for the WT. This paper quantifies the rotor torque control errors and their influence on the power coefficient in partial load operation.

2 Approach

To examine fluctuations in efficiency due to drivetrain speed, torque, temperature, and non-torque-loads (NTLs) an efficiency model for a WT drivetrain is build. This efficiency model of the WT drivetrain is then validated by calibrated measurements gathered on a system test bench. A special 5 MNm torque transducer from PTB with known uncertainty measures the rotor torque. With the calculated rotor torque errors, the impact on the power coefficient is determined.

2.1 Device under test

The study is conducted for the FVA (Forschungsvereinigung Antriebstechnik e. V.) research nacelle. The perfor-

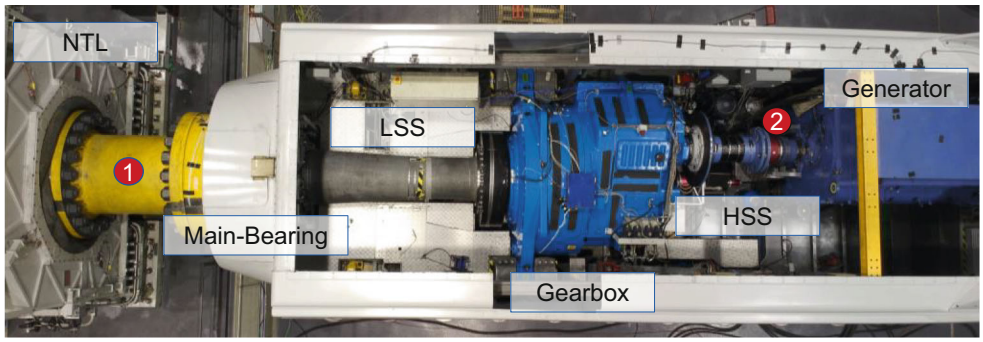

Fig. 7 Drivetrain of the DUT and location of measurement points

mance data of the device under test (DUT) are shown in Table 1.

Among other components the drivetrain of the FVA research nacelle consists of a main bearing, a gearbox and a generator. The gearbox contains a planetary gear stage with three planets and two helical gear stages, resulting in the maximum speed at the HSS of up to 1100 rpm. Within the study the drivetrain efficiency is measured on the system test bench (see Fig. 4) of the CWD.

The test bench is equipped with a 4 MW PMSM permanent magnet synchronous machine (PMSM) prime mover to power the drivetrain. Additionally, the servo-hydraulic non-torque load (NTL) unit provides forces in three and bending moments in two load directions. Combined, the test bench can apply loads in six degrees of freedom. [9]. Overall, the test bench capacity exceeds the limits of the DUT allowing testing of the full operating range.

2.2 Efficiency model for WT drivetrain

The efficiency model consists of existing loss models for the drivetrain components. They enable loss calculations depending on the loads and temperature. The component loads are calculated with an existing validated multi-body-simulation (MBS) model of the nacelle on the testbench (see Fig. 5; [10–12]).

In the model, the losses due to tooth contacts and bearings are considered and implemented in the MBS model. Churning losses in the gearbox and sealing losses were neglected because of their minor influence [13]. The losses considered are displayed in Fig. 6.

The bearing losses are calculated acc. to *Palmgren* [14]. The total frictional torque $T_{fric.}$ of a bearing is the sum of a speed-dependent friction torque T_0 and a load-dependent friction torque T_1.

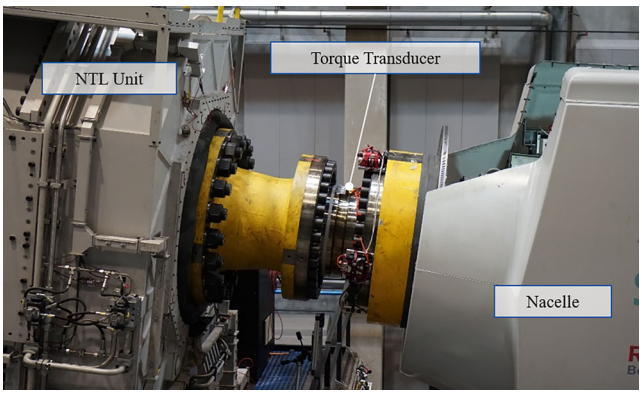

Fig. 8 5 MNm torque transfer standard mounted in the 4 MW test bench at CWD

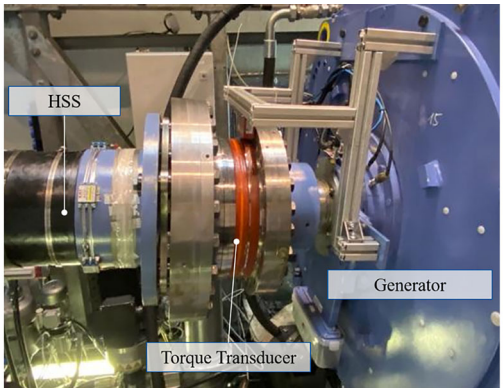

Fig. 9 80 kNm torque transducer on the HSS

$$T_{\text{fric.}} = T_0 + T_1 \tag{5}$$

This approach, in turn is implemented in the calculation model according to FAG [15]. The equations used are shown below. The parameters can be obtained from the bearing catalog.

$$T_0 = f_0 \cdot 10^{-7} \cdot (\nu \cdot n)^{\frac{2}{3}} \cdot d_m^3 \tag{6}$$

$$T_1 = f_1 \cdot P_1 \cdot d_m \tag{7}$$

The friction torque depends on the bearing specific parameters f_0 and f_1, the viscosity ν, the rotational speed n, the bearing diameter d_m and the bearing load P_1. In the MBS model, the rotational speed and load of each individual bearing in the MBS-model are measured at the bearing force element and the resulting friction torques are calculated accordingly. Hereby, losses on the LSS shaft, planetary stage, helical gear stages are considered.

To model the influence of drivetrain temperature on the efficiency the viscosity of the gearbox oil was adapted in the component's loss models. It is assumed that the temperature in the gearbox is homogenous and equal to the sump temperature. In practice the gearbox sump temperature is around 48 °C, on the other hand can reach up to 80 °C, before a shutdown is necessary. Bearings, on the other hand, e.g. at the HSS can reach higher temperatures of up to 90 °C. However, the effects of the local temperature variations mentioned are neglected in this study.

Tooth contact losses are caused by rolling friction and sliding friction on the tooth-flank. As rolling friction losses are comparably low, they are neglected as usual [16]. Sliding friction losses P_{VZP} are calculated using Coulomb's law, from the relative sliding speed $v_g(y)$, the friction coefficient $\mu(y)$, and the normal force on the tooth flank $F_N(y)$ [17] (see Eq. 8)

$$P_{\text{VZP}}(y) = \mu(y) \cdot F_N(y) \cdot v_g(y) \tag{8}$$

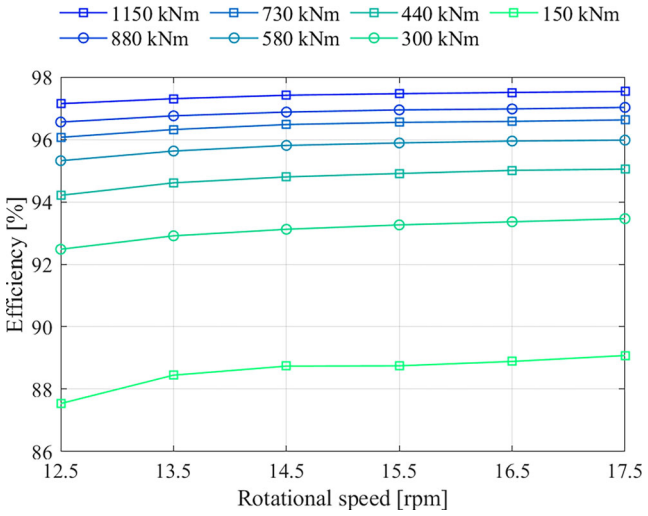

Fig. 10 Measured efficiencies for different drivetrain speeds

All parameters are dependent on the position of the tooth mesh. The relative sliding speed can be calculated using *Linke* [18] and *Niemann* and *Winter* [17] and results in a constant gear loss factor H_V. The friction coefficient μ is simplified as a constant average μ_{mz} over the contact path [19]. For the normal load on the tooth flank, the simplified load distribution defined by *Ohlendorf* is used [20]. Thus, the tooth contact losses are implemented by Eq. 9 as a function dependent of the drivetrain power P_A.

$$P_{\mathrm{VZP}} = \mu_{mz} \cdot P_A \cdot H_V \tag{9}$$

2.3 Experimental test campaign for model-validation

To validate the efficiency model, measurements were performed on the 4 MW system test bench at CWD to validate the efficiency model. Figure 7 shows the drivetrain and the test set up from above. The torque measurement points are located on the LSS (1) and the HSS (2).

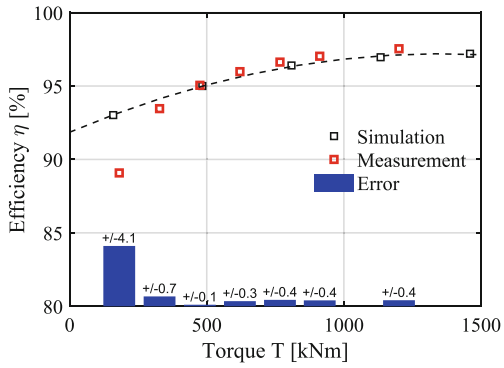

Fig. 11 Comparison of simulated and measured drivetrain efficiency (12.5 rpm, 48 °C)

Table 2 Range of examined NTLs

Hub Load		Range
Bending Moments	M_y	±2000 kNm
	M_z	±2000 kNm
Hub Forces	F_x	0–250 kN
	F_r	0–400 kN

The additionally installed 5 MNm torque transducer used in this work to measure generator torque on the LSS is a hollow-shaft transducer. It measures torque up to 5 MNm using strain gauges. Despite being only calibrated up to 1.1 MNm, it is used as a transfer standard to enable traceable torque measurements in nacelle system test benches. Above 1.1 MNm, it is metrologically characterized using an extrapolation method and assuming a linear behavior based on a linear calibration curve:

$$T_{\mathrm{TTS}} = 3850\,\mathrm{kNm(mV/V)^{-1}} \cdot S_{\mathrm{TTS}} \tag{10}$$

S_{TTS} is the output signal in mV/V and T_{TTS} is the corresponding calibrated torque output in kNm. The expanded relative uncertainty interval ($k=2$) for the linear calibration curve up to 1.5 MNm is 0.290%. Figure 8 shows the torque transducer mounted at the DUT's rotor hub flange.

The torque signal is read out by a high-precision amplifier with a sampling frequency of f_{sample} = 150 Hz and a 50 Hz Bessel filter. To synchronize the autonomous data acquisition system DAQ of the 5 MNm torque transducer to the data acquisition system of the test bench, the test bench's network time protocol (NTP) signal is used for the time stamps of the torque signal. The measured data is transmitted via WLAN using a rotating and a stationary access point. By completing the static torque calibration with additional influences under rotation, the overall relative expanded measurement uncertainty ($k=2$) for rotor

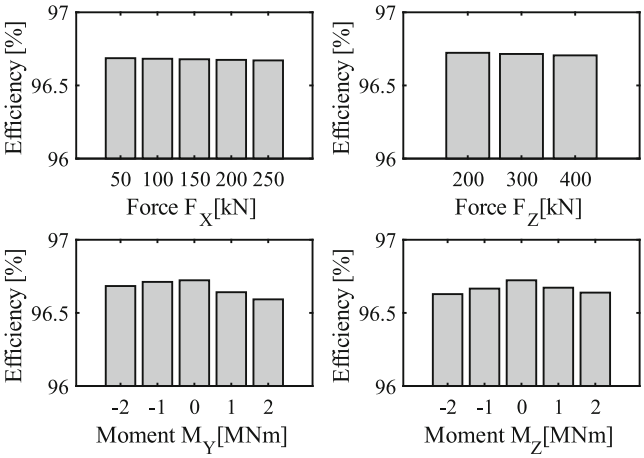

Fig. 12 Influence of NTLs on the drivetrain efficiency

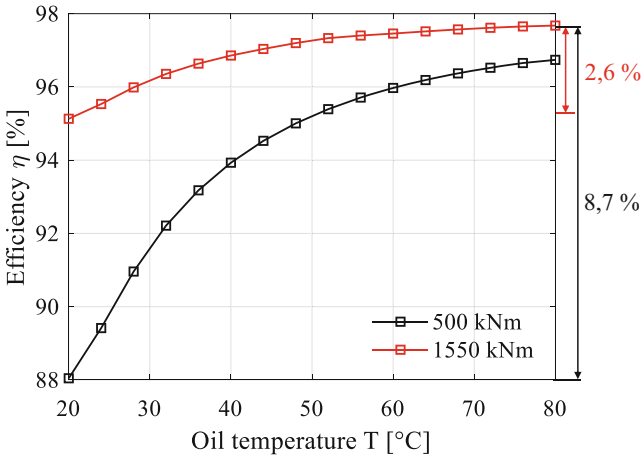

Fig. 13 Drivetrain efficiency for different oil temperatures and torques at 17.5 rpm

torque measurement on the LSS in the test bench was estimated for each load steps. It starts from 0.29% in higher torque range and goes up to 0.65% in lower torque range.

To measure generator torque on the HSS, which is between the gearbox and the generator, an 80 kNm hollow-shaft torque transducer (Fig. 9) is installed. The relation between the measurements output signal S_T of the transducer in kHz and the applied torque T_T in kNm, was defined with the help of a calibration and is described by the following equation:

$$T_T = \frac{2.666\text{kNm}}{\text{kHz}} \cdot S_T \tag{11}$$

The relative expanded measurement uncertainty ($k = 2$) of the transducer amounts to <0.1%. The data is transmitted via the transducer's own telemetry system.

3 Results

First, the variation of the efficiency due to drivetrain torque and speed are examined. For this purpose, the measurements of the 4 MW test-bench are evaluated. The results are then compared to the simulated efficiency to validate the model. Afterwards, the influences of NTLs, and temperature on the drivetrain efficiency are simulative quantified using the efficiency model. Finally, the control error of the rotor torque and the resulting C_p deviation can be determined.

3.1 Influence of the drivetrain torque and speed on the efficiency

Depending on the operating point the WT drivetrain speed and the drivetrain torque varies. The results of the efficiency measurement campaign on the 4 MW test bench for different drivetrain speeds are shown in Fig. 10.

Figure 10 shows that drivetrain efficiency is influenced by the drivetrain speed. At 1150 kNm the deviation between 12.5 rpm and 17.5 rpm is 0.4% while at 150 kNm the difference is 1.6%. From this, it can be concluded that the deviation is small especially in the case of high torques and therefore high powers.

Figure 11 shows the calculated and measured drivetrain efficiency for different drivetrain torques. The chart bars represent the deviation between measurement and simulation.

The modeled efficiency and the measured efficiency match with a deviation of less than 0.7%. The only exception occurs for the simulated value at 170 kNm which shows a deviation of 4.1%. One reason is that for small torques and thus low power, the absolute errors in the loss calculation or measurement have higher impacts. It can be concluded that the model is valid for operation points above a torque of 330 kNm.

Furthermore, the efficiency increases with increasing torque until reaching its maximum asymptotically. Overall, the drivetrain efficiency varies between 94.1% for 330 kNm and 97.1% for 1200 kNm, and therefore has a range of 3%.

Table 3 Summary of rotor torque control errors

Influencing Variable	Conditions	Variable Range	Efficiency Range [%]	
Drivetrain Torque	at 48 °C, 12.5 rpm	300 –1200 kNm	94.1–97.1	<3
Max. efficiency model uncertainty (Torque)	at 48 °C, 12.5 rpm	300–1200 kNm	–	<0.7
Drivetrain Speed	at 1200 kNm	12.5–17.5 rpm	97.1–97.5	<0.4
	at 300 kNm	12.5–17.5 rpm	87.5–89.1	<1.6
NTL (Forces)	F_x F_r	0% ...100%	96.7	<0.01
NTL (Bending moments)	M_y M_z	0% ...100%	96.6–96.7	~ 0.1
Temperature	at 1550 kNm	20 °C...80 °C	95.1–97.7	2.6
	at 500 kNm	20 °C...80 °C	88.0–96.7	8.7
[a]Measurement uncertainty uncalibrated strain gauges	–	0% ...100%	–	5–7*

[a]According to GUY [7]

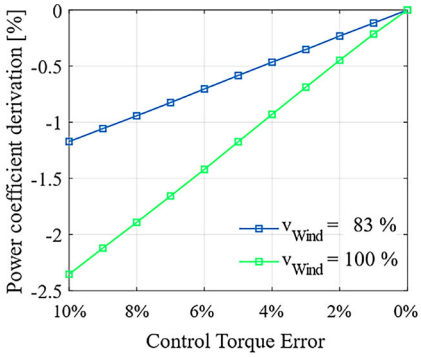

Fig. 14 Influence of rotor torque control errors on the power coefficient at different wind speeds

3.2 Influence of non-torque loads on efficiency

The influence of NTLs on drivetrain losses is examined using the efficiency model. To do this, bending moments around Y-axis (M_y) and Z-axis (M_z), as well as forces in axial (F_x) and radial (F_r) direction were applied to the rotor hub. A realistic load range was determined with a rotor load calculation using blade element theory. The loads investigated are listed in the table below (Table 2.).

The NTLs were changed, while the WT was operated at rated torque and rated speed. (17.5 rpm, 1550 kNm). The results are concluded in Fig. 12.

The efficiency deviations for different hub forces are lower than 0.01%. The bending moments, on the other hand, have a greater effect, but the deviations are still less than 0.1%. The main reason is that NTLs mainly affect the component loads at the main bearing, while the impact on the gearbox loads, where most losses are generated, is small. Therefore, the overall impact of NTLs on the efficiency can be neglected and does not need to be investigated further.

3.3 Influence of drivetrain temperatures on the efficiency

The influences of the temperature variation are simulated with the efficiency model. In Fig. 13 the results are displayed.

Figure 13 shows the efficiency of the drivetrain at rated speed (17.5 rpm) for a relevant torque range between 500 kNm and 1550 kNm, with temperature variation. The deviation in drivetrain efficiency is particularly high at low temperatures. The minimal efficiency is 88.0%, while the maximum efficiency is 97.7%. At rated torque reduction in temperature from 80 °C to 20 °C in the gearbox sump temperature leads to an efficiency reduction of up to 2.6%. At a lower torque of 500 kNm this difference is up to 8.7%. The main reason are churning losses that decrease with higher temperatures. Additionally, churning losses have greater impacts on efficiency at lower torque, because they are only dependent on speed that was constant for this analysis. It can be concluded that the influence of the temperature on drivetrain efficiency is significant and should be further examined.

3.4 Summary of the resulting control torque errors

As shown in the previous section's efficiency varies depending on drivetrain speed and torque, NTLs, and temperature. Since in WTs controls typically constant efficiencies at rated speed and rated torque are used to calculate the rotor torque, the variations of the efficiency represent the error in the rotor torque control. As a reference the direct measurement of rotor torque measurement uncertainty for in field measurements with uncalibrated strain gauges is used. Finally, the influence of the efficiency model uncertainty on the rotor torque control is evaluated. All influences on control torque errors are summarized in the following Table 3.

For the experimentally investigated variables drivetrain torque and speed, the control torque errors were based on the reference torque measurement on the LSS, which's measurement uncertainty is 0.29% in higher torque range and 0.65% in lower torque range. The uncertainty range is sufficient to guaranty a valid determination of the rotor torque control errors.

The measurement results show that the rotor torque control error can reach up to 10%. As a conclusion influence of rotor torque control errors on the power coefficient needs to be further examined.

3.5 Influence of rotor torque control errors on the power coefficient

Using an aerodynamic model of the rotor, the influences of rotor torque control deviations are examined. Rotor load simulation is done by means of MBS using blade element theory as it is implemented in the AeroDyn force element code [21]. The loads acting on the rotor blades are calculated within respect to local wind speed and wind direction given by turbulent wind fields, which were generated using TurbSim [22]. The Rotor model is generic but shows realistic behavior. To estimate the influence on the power coefficient, first simulations were performed with OTC and the maximum power coefficient $C_{p,max}$ is calculated. Then the rotor torque is to simulate the torque control errors. The result is shown in Fig. 14.

The calculations were carried out at different windspeeds between 83% and 100% rated wind speed. Those operating points represent the partial load range of the WT examined, in which the influence on the power output is most relevant. At higher torque deviations the power output

is lower than expected. For 83% of rated wind speed and a rotor torque control error of 10% the power output is reduced by 1.2% at the respective operation point. For 100% rated wind speeds the deviation is 2.4%.

4 Conclusions

In this paper an efficiency model for WT drivetrains was developed, which is based on existing component efficiency models. This model was validated with measurements at different operation points on a system test bench. The validated model was used to quantify the influences of drivetrain torque and speed on the efficiency. Furthermore, influences of NTLs and temperature on the drivetrain efficiency were simulated. On the basis of the results the influence of the rotor torque control error on the power coefficient was simulated.

Key findings of the paper:

- The drivetrain efficiency was simulated with an accuracy of up to 0.7%. This accuracy is sufficient for most applications and slightly above the measurement uncertainty range of 0.65%. Thus, the simulation is valid for use in the assessment of this paper.
- The efficiency calculation model shows that NTLs have no significant influence on the drivetrain efficiency since most of the losses appear in the gearbox and NTLs are mainly carried by the main bearing. Therefore, NTLs can be neglected for efficiency models.
- The efficiency model results show that the temperature has a major impact on the drivetrain efficiency.
- The variations in drivetrain efficiency lead to errors in rotor torque control. The influence of the rotor torque control error on the power coefficient was determined using an aerodynamic rotor model. The power coefficient decreased by up to 2.4%.

In the future the efficiency model needs to be validated in terms of varying temperature. In addition, the occurrence of load cases and temperature in field operation must be considered. This allows us to assess the impact of the decrease of power coefficient on the total energy production of the WT.

Finally, it can be concluded that the significant errors in rotor torque control result in suboptimal turbine control. Reducing the WT's power coefficient leads to lower annual energy production, and higher LCOE. An optimized prediction of the drivetrain efficiency, by modeling or test bench measurements, can reduce the rotor torque control errors and ultimately the LCOE.

Acknowledgements The project 19ENG08 – WindEFCY has received funding from the EMPIR program co-financed by the Participating States from the European Union's Horizon 2020 research and innovation program. The input of all project partners and of my colleagues is gratefully acknowledged.

EMPIR EURAMET
The EMPIR initiative is co-funded by the European Union's Horizon 2020 research and innovation programme and the EMPIR Participating States
WindEFCY

Funding Open Access funding enabled and organized by Projekt DEAL.

References

1. Burton T et al (2021) Wind energy handbook. Wiley, Hoboken
2. Rohatgi J, Vaughn N (1994) Wind Characteristics: an analysis for the generation of wind power. Alternative Energy Institute
3. Elosegui U et al (2018) Pitch angle misalignment correction based on benchmarking and laser scanner measurement in wind farms. Energies 11(12):3357
4. Gasch R, Twele G (2005) Windkraftanlagen, 4th edn. Teubner, Wiesbaden
5. Manwell JF et al (2010) Wind energy explained: theory, design and application. Wiley, Hoboken
6. Hau E (2016) Windkraftanlagen. Springer, Berlin Heidelberg
7. Guy B et al (2015) Measurement and traceability of torque on large mechanical devices. In: Proceedings SENSOR
8. Weidinger P et al (2021) Need for a traceable efficiency determination method of nacelles performed on test benches. Meas Sensors 18:100159
9. Liewen C, Radner D, Jacobs G, Schelenz R, Bosse D (2015) New infrastructure and testprocedures for analyzing the effects of wind and grid loads on the local loads of wind turbines on a system test bench. Proc. Conf. for Wind Power Drives, CWD2017, Aachen, pp 241–254
10. Matzke D, Jacobs G, Schelenz R (2017) Full scale system simulation of a 2.7 MW wind turbine. J Physics Conf Ser Vol 1037(6): 241–254
11. Matzke D, Jacobs G, Schelenz R (2019pp) Validation of MBS modeling methods to calculate bearing and tooth loads in the planetary gear stage of a wind turbine. Proc. Conf. for Wind Power Drives, CWD2019, Aachen, pp 333–347
12. Matzke D et al (2018) Validation of the gearbox load calculation of a wind turbine MBS model. J Phys Conf Ser 1037:62025
13. FVA (2017) Verlustleistung von Stirnradverzahnungen – Experimentelle Untersuchung der Verlustleistung von Stirnradverzahnungen. Forschungsvorhaben Nr. 686 I Heft 1223
14. Palmgren A (1957) Neue Untersuchungen über Energieverluste in Wälzlagern. VDI-Berichte, vol 20

15. Schaeffler (2006) INA/FAG Wälzlagerkatalog
16. FVA (2017) Abschlussbericht, Verlustleistung von Stirnradverzahnungen. Heft 1223
17. Niemann G, Winter H (2003) Getriebe allgemein. Zahnradgetriebe – Grundlagen, Stirnradgetriebe, 2nd edn. Maschinenelemente, vol 2. Springer, Berlin
18. Linke H (1996) Stirnradverzahnung: Berechnung, Werkstoffe, Fertigung. Hanser, München
19. Doleschel A (2001) Wirkungsgradtest. FVA-Forschungsheft Nr. 664
20. Ohlendorf, H., Verlustleistung und Erwärmung von Stirnrädern, Dissertation TU München, (1958)
21. NREL Homepage. https://www.nrel.gov/wind/nwtc/turbsim.html. Accessed 9 Mar 2020
22. NREL Homepage. https://www.nrel.gov/wind/nwtc/aerodyn.html. Accessed 9 Mar 2020